COBEM 2023 27TH INTERNATIONAL CONGRESS OF MECHANICAL ENGENEERING

ABCM Brazilian Society of Mechanical Sciences and Engineering
27th ABCM International Congress of Mechanical Engineering
December 04-08, 2023, Florianópolis-SC, Brazil

COB-2023-0682
ANALYSIS OF THE PRESSURE FIELD IN ARTERIOVENOUS FISTULA

Lucas Matheus Silva da Penha
Willyam Brito de Almeida Santos
Federal University of Rio Grande do Norte, Department of Mechanical Engineering, Center of Technology, Laboratory of Fluid Mechanics, Avenue Senador Salgado Filho, 300 – Lagoa Nova, CEP 59078-970 – Natal/RN
lucas.matheus.056@ufrn.edu.br
willyambas@gmail.com

Jonhattan Ferreira Rangel
ferreira.rangel.095@ufrn.edu.br

Sabrina Machado Santos
sabrina.machado.033@ufrn.edu.br

Allan Pedro Silva dos Santos
allanpedro.sds@gmail.com

Kleiber Lima De Bessa
klbessa@ct.ufrn.br

Abstract. *Hemodialysis is the best treatment for patients with chronic renal failure. To perform this treatment it is necessary to design a vascular access (VA). One of the common complications in arteriovenous fistula (AVF) is steal syndrome, due to the detour of arterial blood to the AVF and not to the peripheral limbs of the patient's. This study analyzed the pressure field and flow conditions in an arteriovenous fistula model (in vitro) subjected to the conditions of steal syndrome on a permanent experimental bench. For the completion of the work, an ideal AVF was modeled and manufactured with pressure acquisition points in the distal and proximal arterial regions, anastomosis, and venous region. Following this stage, the AVF with a 45° anastomosis angle (AA) was fabricated using 3D printing.For the experimental analysis pressure transducers were used MPX5050DP, ball valves 1/3", flow sensor USN-HS41TA, diaphragm motor pump S-60-12, Arduino UNO/NANO e ESP 32 LoRa. The AVF was submitted to 2 flow configurations: configuration A, a flow with a maximum mean flow rate equal to 2163.26 ml/min in the proximal artery and zero flow rate in the distal artery, and configuration B, in which a flow rate of 70% of the maximum mean flow rate was applied in the proximal artery and 30% in the distal artery. In the experiments, for A, the pressure differential varied from 14,20 kPa at P1 (Pressure Point 1) at the entrance to the proximal artery to 1,00 kPa at P5 (Pressure Point 5) at the exit of the venous segment. For B, the pressure varied from 11,65 kPa at P1 to 1,20 kPa at P5. It can be inferred that the AA is the cause of most of the energy dissipated in the flow, as the sudden change in geometry at the anastomosis causes the flow to separate.*

Keywords: *Arteriovenous Fistula, Pressure drop, Steal syndrome, Anastomosis Angle, Flow rate.*

1. INTRODUCTION

Hemodialysis (HD) is the best treatment for patients with chronic renal failure. For the completion of this treatment, a vascular access (VA) is needed, being the arteriovenous fistula (AVF) the most recommended due to better flow conditions and lower complication rates when compared to other types of VA. The AVF is a connection between an arterial and a peripheral venous vessel made by a vascular surgeon, allowing blood to be filtered by a dialyzer. AVFs are preferred as they present less complications and have lower infection rates (ALAM. *et al.,* 2022). One of the common complications in AVF is steal syndrome (SD), in which this syndrome will be analyzed through the pressure field of the system. Steal syndrome is a complication that may occur in 4% of patients with AVFs (PLUMB, TROY J. *et al.,* 2008). The study by ZAMANI; KAUFMAN; KINLAY (2009) points out that it can occur in 70% of radiocephalic fistulas and in 90% of brachial artery fistulas.

In this context, the arteriovenous fistula acts as a low resistance, high compliance pathway between the high pressure arteries and the low pressure venous system. This atypical communication causes a small change in hemodynamics in the vascular system. The study of hemodynamics has been recognized as an important role in the development of the study of AVFs (PROUSE *et al.,* 2020). The syndrome is clinically characterized by paresthesias, pain, stiffness of fingers, diminished pulses in the distal vasculature, and (in the most serious cases) gangrenous/necrotic events. (BABAKHANI; JINDAL, 2014). According to PLUMB, TROY J. *et al.,* (2008) SD is defined when blood flows from the high-resistance circulation distal to the anastomosis to the low-resistance fistula outlet. Due to the blood flow not conducting properly to the peripheral limbs of the patient, several problems occur, for example: Thrombosis, infection, pseudoaneurysm and distal ischemia.

However, symptoms of hand ischemia(pain, parasthesia, or gangrene) only occur in 1–2% of radiocephalic fistulae and 5–10% of bra-chial artery fistulae. (ZAMANI; KAUFMAN; KINLAY, 2009). The options for treatment of steal syndrome include complete ligation of the AVF (thus abolishing access), revision of the anastomosis to a more distal site, distal revascularization and interval ligation, plication, and banding (BABAKHANI; JINDAL, 2014). In this setting, understanding the hemodynamics of blood flow in the AVF is essential and is often neglected, leading to other surgical interventions for correction (VAN CANNEYT *et al.,* 2010). It is understood that inadequate construction of the AVF can lead to insufficient blood flow for the HD procedure. *In vitro* studies are complex due to the geometric conditions of the AVF so the application of Fluid Mechanics to the study of the AVF has increased mainly due to the better understanding of the pressure field and flow of the flow taking place in the system.

Studies using *in vitro* models in the AVF have been used and have become relevant due to their excellent results. This work aims to study the pressure field effects in an ideal rigid AVF subjected to conditions of distal ischemia due to steal syndrome, with flow variation in the proximal artery, distal artery and venous segment. In this way, it will be possible to study the consequences of this syndrome in patients with chronic renal failure, with a view to quality of life and well-being.

2. MATERIALS AND METHODS

The AVF used for the methodology was the *in vitro* model. The experimental bench was designed to create a permanent flow in the AVF. It was developed at the Laboratory of Fluid Mechanics - LFM of the Federal University of Rio Grande do Norte (UFRN), in order to capture pressure and flow data at established points in the system. The bench assembly was organized into four sections: Control, Test, Sensors and Data. Figure 1 below shows the steps for the realization of this work.

Figure 1. Schematic flowchart of the methodology

2.1 SECTIONS

The function of the Control Section is responsible for achieving permanent flow. This partition has the function of regulating the fluid pressure and flow, from the developed programs and entered data. The materials used are: Arduino UNO, power circuit, locked font 12V e Motor Pump RHONDAMAQ - CF-2201[a].

The Test section has the function of promoting flow in the AVF, and it is here that the pump operates, taking working fluid from the reservoir and circulating it through the valves, connections, sensors, and the AVF *in vitro*. The

materials used in this section were: stainless steel tank, Polyvinyl Chloride (PVC). For the connection to the proximal artery, hoses 3 mm thick and 5 mm in diameter were used, and for the connection to the vein, hoses 2 mm thick and 7 mm in diameter were used. Two ball valves were used 1⁄3″ named V1 and V2, and the AVF model *in vitro*.

The Sensors section is responsible for reading and processing the output signals from the pressure and flow sensors. The materials used in this section were: Pressure sensor MPX5050DP, Flow Sensor YF-S401, ESP32 - LoRa and Arduino Nano. The flow sensor measures the flow by counting the revolutions of the internal turbine.

The Data section is responsible for calibrating, preparing and implementing the input and output data for system operation, as well as receiving the data resulting from the system's pressure and flow sensors. A computer was used with the Arduino IDE software and Excel. Figure 1 below shows.

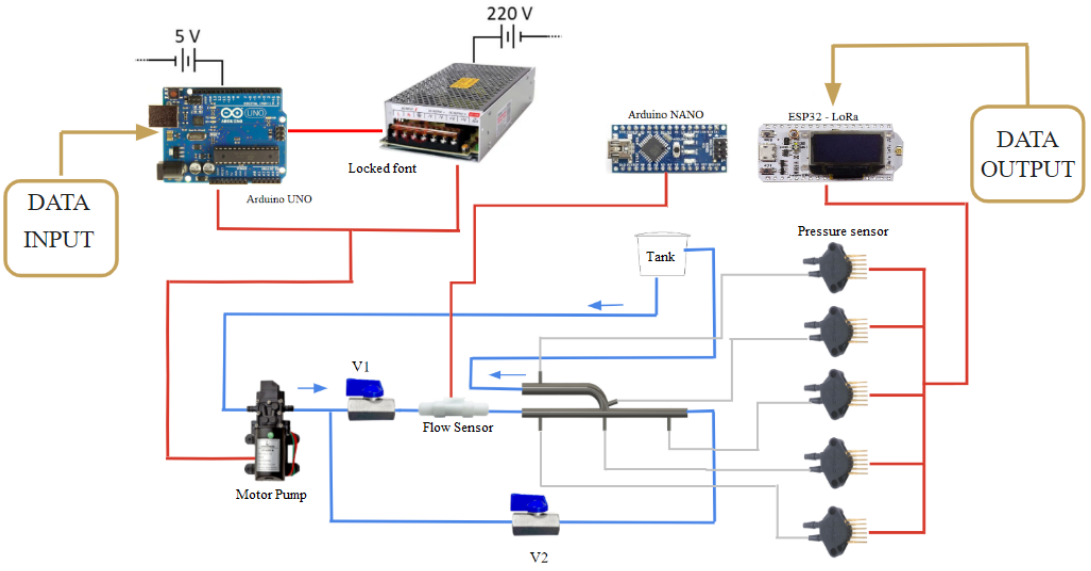

Figure 2. Schematic of the experimental bench

2.2 AVF MODELING

The AVF was designed with 4 mm in diameter in the artery and 6 mm in diameter in the venous segment, it has 5 pressure ports with 2 mm diameter and installed in the following segments: P1 (Pressure 1) at the entrance in the proximal artery, P2 (Pressure 2) on the wall of the artery opposite the anastomosis, P3 (Pressure 3) in the distal artery, P4 (Pressure 4) at the start of the venous segment and P5 (Pressure 5) at the exit of the venous segment. For anastomosis, 6 mm in length and 4 mm in width were considered. Points P2 and P3 were placed in these regions with the intention of detecting the presence of flow disturbances through pressure. Figure 3 shows schematically.

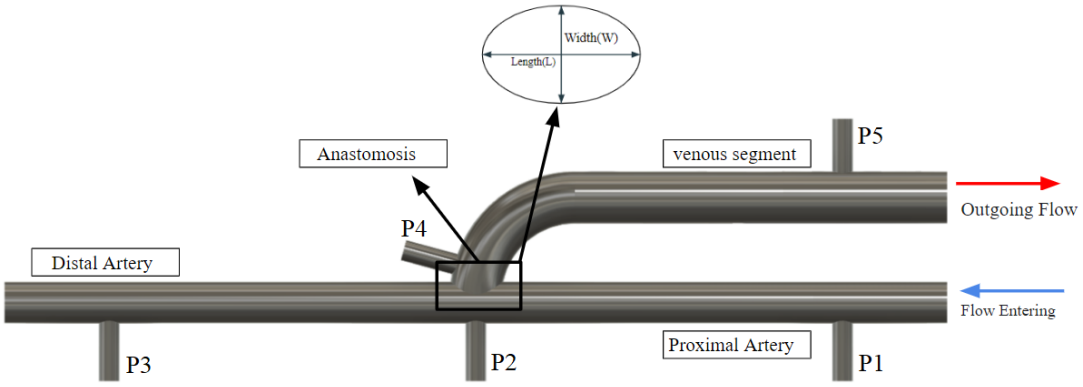

Figure 3. AVF and its Pressure Points.

The AVF drawings were created using Fusion 360 software (Autodesk), changed and exported in Standard Triangle Language (STL). The STL file enabled the creation of the volumetric triangular mesh from the outer shell for 3D

printing, so the technique that was used for printing is Fused Deposition Modeling (FDM). The AVF was developed by extruding a filament of Acrylonitrile Butadiene Styrene (ABS) thermoplastic material in a da Vinci 1.0 Pro model printer. For this work, the AVF was submitted to 2 flow configurations: configuration A, a flow with an average flow rate equal to 2163.26 ml/min in the proximal artery and zero in the distal artery, in which simulates the AVF without steal syndrome. Configuration B, a flow with 70% of the mean flow value in the proximal artery and 30% in the distal artery was applied and in this model, the steal syndrome is performed. The engine load for this job was 80%. As shown in figure 4.

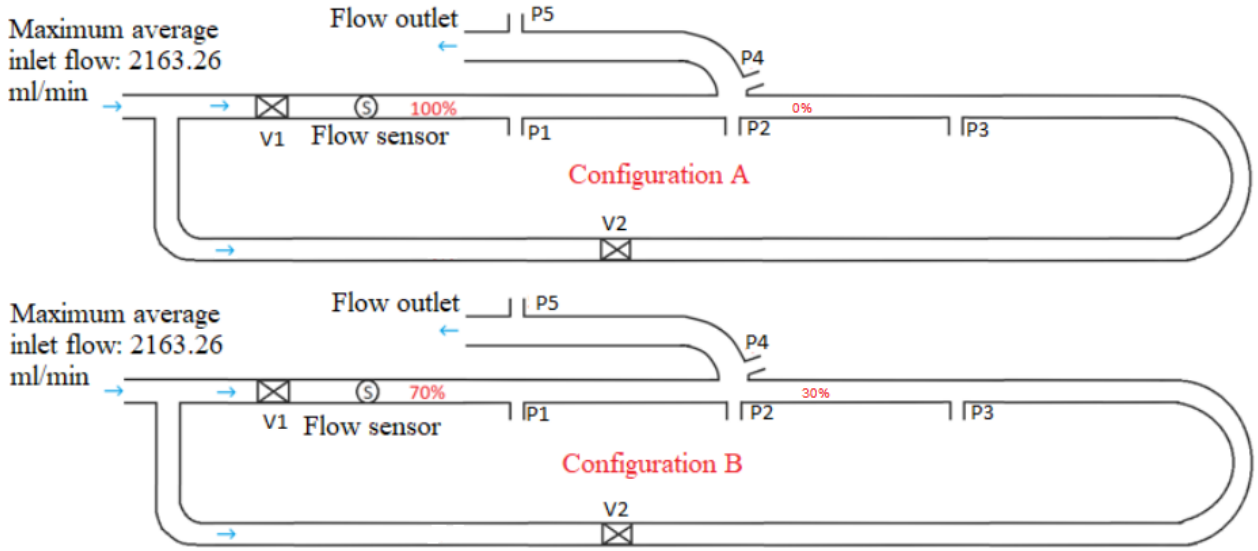

Figure 4. Schematic of the AVF without and with Steal Syndrome

3. RESULTS AND DISCUSSIONS

In this *in vitro* study, some differences in hemodynamics were identified regarding configurations A and B. Table 1 shows that throughout the flow there is a decreasing behavior in the pressure parameters. Configuration A shows a maximum pressure of 14,20 kPa and a minimum of 1,00 kPa. Configuration B shows a maximum pressure of 11,65 kPa and a minimum pressure of 1,20 kPa.

Points	P1	P2	P3	P4	P5
Configuration A[kPa]	14,20±0,20	12,25±0,15	12,60±0,20	7,00±0,40	1,00±0,20
Configuration B[kPa]	11,65±0,75	10,50±0,40	10,90±0,40	5,70±0,20	1,20±0,20

Table 1 - Pressure values for Configuration A and B

At point 1, the pressure was 14,20 kPa (with a standard deviation of 0,20) and configuration B 11,65 kPa (with a standard deviation of 0,75).

At point 2, the pressure was 12,25 kPa (with a standard deviation of 0,15) and configuration B 10,50 kPa (with a standard deviation of 0,40).

At point 3, the pressure was 12,60 kPa (with a standard deviation of 0,20) and configuration B 10,90 kPa (with a standard deviation of 0,40).

At point 4, the pressure was 7,00 kPa (with a standard deviation of 0,40) and configuration B 5,70 kPa (with a standard deviation of 0,20).

At point 5, the pressure was 1,00 kPa (with a standard deviation of 0,20) and configuration B 1,20 kPa (with a standard deviation of 0,20).

Using P1 as a reference, it is possible to measure the pressure drops at each point. Therefore, for configuration A, the maximum pressure drop is between P1 and P5, which was 13,20 kPa and the minimum was between P1 and P3, which was 1,60 kPa. For configuration B, the maximum pressure drop was 10,45 kPa and the minimum was 0,75 kPa. Table 2 below shows these results.

Points	$\Delta P_{P1\text{-}P2}$	$\Delta P_{P1\text{-}P3}$	$\Delta P_{P1\text{-}P4}$	$\Delta P_{P1\text{-}P5}$
Configuration A[kPa]	1,95	1,60	7,20	13,20
Configuration B[kPa]	1,15	0,75	5,95	10,45

Table 2. Pressure Differential of Configuration A and B

Analyzing configuration A, it can be inferred that because the flow is more intense in the proximal artery and zero in the distal artery, the pressures P1, P2, P3 and P4 are higher than in configuration B. When P2 and P3 are analyzed, it can be seen that there was no great change in pressure, inferring that there are no major disturbances, as the pressure fell due to the distributed pressure drop. For P4, there is a sudden drop in pressure, it is likely that this drop in pressure could be caused by the geometry of the anastomosis, as P4 is located in the AA. At P5, the lowest pressure value is found, as the AA causes a large localized pressure drop.

Analyzing configuration B, it can be inferred that because the flow is less intense in the proximal and distal arteries, the pressures P1, P2, P3 and P4 are lower than in configuration A. When analyzing P2 and P3, the pressure dropped due to the distributed pressure drop. For P4, there is a sharp drop in pressure due to the AA. At P5, the lowest pressure value is found, as the AA causes a large localized pressure drop.

Studying both configurations, the pressures P1, P2, P3 and P4 in configuration A are higher than in configuration B, due to the configuration adopted for the *in vitro* experiment. P4 is the most critical point, as it is in a curved region of the system, so the flow is subject to stricter flow conditions. It is known that when the flow moves towards the venous segment, it has a very abrupt change of direction, causing recirculation zones, implying major disturbances. At P5, the pressure of configuration B is higher. This may have been due to the methodology adopted for theft syndrome for this work, i.e. when analyzing the outlet flow of both configurations, they are the same. Another explanation could be the absence of disturbances or disturbances without intensity capable of significantly altering the pressure around P5. Graph 1 shows the comparison between A and B.

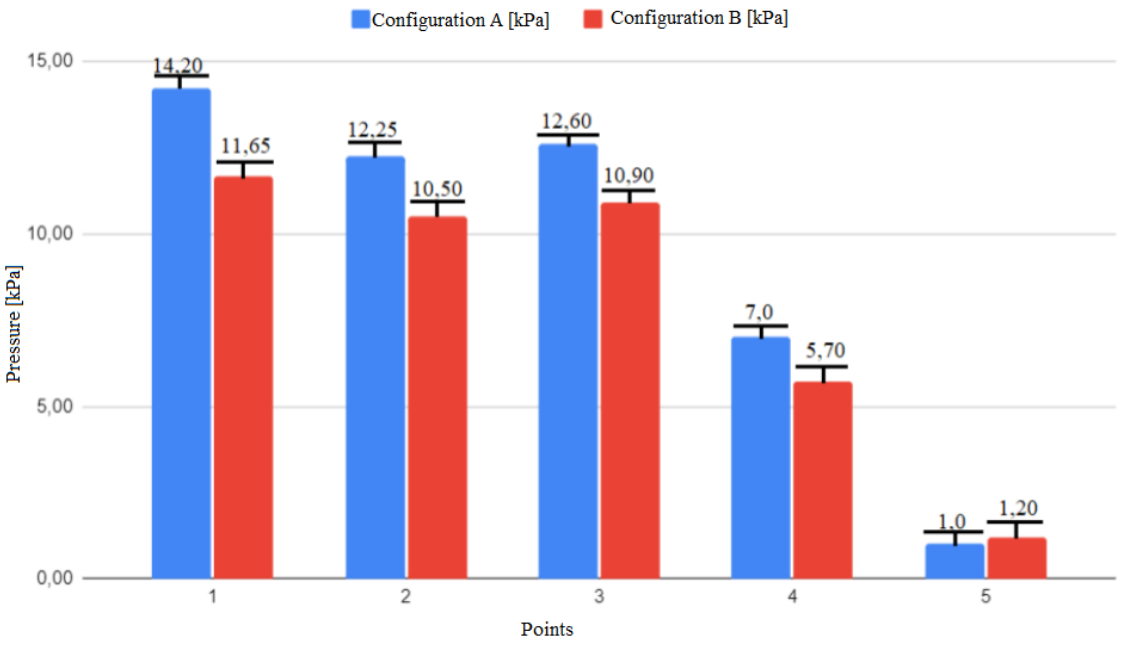

Figure 5. Comparison of Configuration A and B Pressures.

The work of BOTTI et al. (2013), which compared *in vitro* and *in silico* models, in it the pressure drop as a function of flow rate is presented. The study becomes significant because it indicates a large dependence of the pressure drop on the flow rate and the change due to instabilities in the AVF.

The study by SANTOS (2022) states that in a AVF the main disturbances that influence pressure drop are: points of separation of the flow at the proximal anastomotic junction as the fluid enters the anastomosis; formation of a vortex

with counterclockwise rotation and collision of thDe fluid on the external wall of the vein between the distal anastomotic junction forming a large vortex with clockwise rotation that occupies much of the anastomosis. The pressure drop in an AVF is closely linked to instabilities arising at the anastomosis and is considered a global indicator of the total hemodynamic dynamics of a fistula (BROWNE *et al.,* 2015).

4. CONCLUSION

Thus, it is possible to understand through the results that the variations presented between the pressures of both configurations, is that the AA is the major cause of the dissipated energy of the flow, because the sudden change of geometry in the anastomosis causes flow separation point, causing: disturbances in the flow, generation of recirculation zones in the internal wall of the vein and stagnation points. In this way, recirculation weakens the effective area for main stream flow, accelerating the fluid particles and lowering the pressure.

Finally, this study emphasizes the importance and care that must be taken with the construction of the AVF, as surgical techniques can be used to modify the fistula or the flow toward the patient's peripheral limbs, successfully treating the steal syndrome and preserving the fistula.

5. REFERENCES

AMATO, A. Fístula arteriovenosa para Hemodiálise. Disponível em:<https://vascular.pro/fistula-arteriovenosa-para-hemodialise-fav/> . Acesso em: 17 Junho de 2023.

AN TRICHT, I.; WACHTER, D.; TORDOIR, J.; VEERDONCK, P. Hemodynamics and complications encountered with arteriovenous fistulas and grafts as vascular access for hemodialysis: A review. Annals of Biomedical Engineering, v. 33, n. 9, p. 1142–1157, 2005.

BABAKHANI,A.; JINDAL, RAHUL M. Tube Banding to Correct Steal Syndrome after Arteriovenous Fistula Construction for Hemodialysis. Sage Journals.V. 80, 2014.

BOTTI, L. CANNEYT, K. V.; KAMINSKY, R.; CLAESSENS, T.; PLANKEN, R. N.; VERDONCK, P.; REMUZZI, A.; ANTIGA, L. Numerical Evaluation and Experimental Validation of Pressure Drops Across a Patient-Specific Model of Vascular Access for Hemodialysis. Cardiovascular Engineering and Technology. v. 4, n. 4, p. 485–499, 2013.

BROWNE, L. D. et al. In vivo validation of the in silico predicted pressure drop across an arteriovenous fistula.National Library of Medicine.2015.

ENE-IORDACHE, B.; MOSCONI, L.; REMUZZI, G.; REMUZZI, A. Computational fluid dynamics of a vascular access case for hemodialysis. Journal of Biomechanical Engineering, v. 123, n. 3, p. 284–292, 2001.

ENE-IORDACHE, B.; CATTANEO, L.; DUBINI, G.; REMUZZI, A. Effect of anastomosis angle on the localization of disturbed flow in “side-to-end” fistulae for haemodialysis access. Nephrology Dialysis Transplantation, v. 28, n. 4, p. 997–1005, 2013.

FOX, R. W.; MCDONALD, A.; PRITCHARD, P. Introdução à Mecânica dos Fluidos. 6. ed. [s.l.] LTC - Livros Técnicos e Científicos Editora LTDA, 2015.

N. ALAM; M. WALSH; D. NEWPORT. Experimental evaluation of a patient specific Brachio-Cephalic Arterio Venous Fistula (AVF): Velocity flow conditions under steady and pulsatile waveforms. Science Direct. V. 106, 2022.

PLUMB, T. J.; LYNCH, T. G. ; ADELSON, A. B. Treatment of steal syndrome in a distal radiocephalic arteriovenous fistula using intravascular coil embolization. Science Direct. V. 47, Pages 457-459, 2008.

PROUSE, G;STELLA, S.; VERGARA, C.;QUARTERONI, A.; ENGELBERGER, A.; CANEVASCINI, R.; GIOVANNACCI, L. Computational Analysis of Turbulent Hemodynamics in Radiocephalic Arteriovenous Fistulas to Determine the Best Anastomotic Angles. Science Direct. V. 68, Pages 451-459, 2022.

RAMUZAT, A.; HOW, T. V.A. ; BAKRAN, A. Steal phenomenon in radiocephalic arteriovenous fistula. *In vitro* haemodynamic and electrical resistance simulation studies. Science Direct. V.25, , p. 246-253, 2003.

SANTOS, Willyam Brito de Almeida. Análise do escoamento pulsátil em fístula arteriovenosa com variação do ângulo de anastomose in vitro e in silico. 2021. 122f. Dissertação (Mestrado em Engenharia Mecânica) - Centro de Tecnologia, Universidade Federal do Rio Grande do Norte, Natal, 2021.

SIVANESAN, S.; HOW, T. V.; BLACK, R. A.; BAKRAN, A. Flow patterns in the radiocephalic arteriovenous fistula: An *in vitro* study. Journal of Biomechanics, v. 32, n. 9, p. 915–925, 1999.

SILVA, J. DE A.; KARAM-FILHO, J.; BORGES, C. C. H. Computational Analysis of Anastomotic Angles by Blood Flow Conditions in Side-to-End Radio-Cephalic Fistulae Used in Hemodialysis. Journal of Biomedical Science and Engineering, v. 08, n. 03, p. 131– 141, 2015.

VAN CANNEYT, K.; POURCHEZ, T.; ELOOT, S.; GUILLAME, C.; BONNET, A.; SEGERS, P.; VERDONCK, P. Hemodynamic impact of anastomosis size and angle in side-toend arteriovenous fistulae: A computer analysis. Journal of Vascular Access, v. 11, n. 1, p. 52–58, 2010.

ZAMANI, P. ; KAUFMAN,J. ; KINLAY, S. Ischemic steal syndrome following arm arteriovenous fistula for hemodialysis. Sage Journals.V. 14, 2009.

6. RESPONSIBILITY NOTICE

The author(s) is (are) the only responsible for the printed material included in this paper.